Available online at www.sciencedirect.com
SCIENCE DIRECT
Polymer 46 (2005) 6682–6694
polymer
www.elsevier.com/locate/polymer

PolyHIPE: IPNs, hybrids, nanoscale porosity, silica monoliths and ICP-based sensors

Michael S. Silverstein*, Huiwen Tai, Anatoly Sergienko, Yulia Lumelsky, Svet Pavlovsky

Department of Materials Engineering, Technion-Israel Institute of Technology, Haifa 32000, Israel

Available online 6 June 2005

Abstract

Typical polyHIPE (porous polymers from high internal phase emulsions) have a cellular structure with volume fractions from 0.2 to 0.04, cell diameters from 15 to 25 μm and intercellular pore diameters from 0.5 to 10 μm. Unique interpenetrating polymer networks synthesized within the polyHIPE exhibited enhanced mechanical properties and an extended temperature range for damping. Hybrid polyHIPE that combine an inorganic polysilsesquioxane network with an organic polystyrene network exhibited superior high temperature mechanical properties and enhanced thermal stability. A nanoscale porosity in the cell walls, produced through the addition of a porogen to the HIPE, reduced the density and significantly enhanced the specific surface area. Porous silica monoliths with silica volume fractions of as low as 0.02 were produced through the pyrolysis of hybrid polyHIPE. PolyHIPE coated with an intrinsically conducting polymer exhibited reversible and repeatable changes in conductivity on exposure to acetone vapor, demonstrating their potential as sensor materials.

Keywords: Hybrid high internal phase emulsion polymer (polyHIPE); Interpenetrating polymer networks (IPN); Intrinsically conducting polymer (ICP)

1. Introduction

1.1. Polymerized high internal phase emulsions

A high internal phase emulsion (HIPE) is an emulsion in which the dispersed phase occupies from 74 to 96% of the volume [1,2]. Of particular interest are HIPE in which the major, dispersed phase consists of water containing a water-soluble polymerization initiator and the minor, continuous phase consists of monomers and an emulsifier. The monomers in the continuous phase can then be polymerized to yield a porous polymer, a polyHIPE, with a low polymer volume fraction [3]. The cellular structure of a polyHIPE is isotropic and quite different from the oriented structure of commercial blown and extruded foams. The use of polymers as absorbents for the removal of contaminants from water is being investigated [4,5]. PolyHIPE, with their porous structure, have demonstrated advantageous structural properties and absorbency for use as absorbents [6–10]. PolyHIPE have also been used in ion exchange systems [11,12] and as heat resistant structural foams [13–16]. PolyHIPE can be synthesized from a wide variety of monomers and have a wide range of potential applications. This paper will describe a variety of polyHIPE-based material systems and polyHIPE applications including interpenetrating polymer networks (IPN), hybrid polyHIPE, polyHIPE with nanoscale porosity, silica monoliths, and sensors from polyHIPE coated with intrinsically conducting polymers (ICP).

1.2. Interpenetrating polymer networks

Polymeric materials with a wide temperature range for damping can be produced through the synthesis of IPN from two incompatible polymers with widely separated glass transition temperatures (T_gs) [17–22]. Sequential IPNs can be synthesized by swelling a crosslinked polymer I with monomer II that contains a crosslinking co-monomer and an initiator, and then polymerizing and crosslinking monomer II. PolyHIPE are crosslinked, porous polymers whose damping capabilities can be enhanced by using them as the basis for the synthesis of sequential IPN [23]. If polymer II has a higher T_g than polymer I then the high temperature mechanical properties of the polyHIPE will be enhanced.

* Corresponding author. Tel./fax: +972 4 829 4582.
E-mail address: michaels@tx.technion.ac.il (M.S. Silverstein).

0032-3861/$ - see front matter © 2005 Elsevier Ltd. All rights reserved.
doi:10.1016/j.polymer.2005.05.022

1.3. Hybrids and silica monoliths

Several high temperature polyHIPE have been investigated: the copolymerization of *N*-substituted maleimide and bismaleimide [14–16] and the copolymerization of a maleimide-terminated aryl ether sulfone macromonomer using a non-aqueous HIPE [24]. Polysilsesquioxanes (SSQ) have attracted much attention for their extraordinary heat and fire resistance [25]. They are most broadly described by an empirical formula $(RSiO_{1.5})_n$, where R is an alkyl group or hydrogen. SSQ can be prepared from the hydrolytic condensation of organotrialkoxysilanes [26], $RSi(OR')_3$ or $RSiX_3$, where R' is an organic group and X is a halogen. Hybrid materials can be synthesized from the combination of an organic polymer with an SSQ-like network [27,28]. A hybrid polyHIPE, a polyHIPE containing a polysilsesquioxane network, can be produced through the addition of an organotrialkoxysilane that contains vinyl groups for free radical polymerization and/or copolymerization during polyHIPE synthesis [29]. The polymer chains have an organic backbone and are crosslinked by a polysilsesquioxane network formed by the hydrolysis and condensation of the pendent alkoxysilyl groups. It has been shown that pyrolysis of a hybrid polyHIPE can yield a silica monolith with a cellular structure similar to that of the original polyHIPE [30].

1.4. Sensors and intrinsically conducting polymers

There is a pressing need to provide reliable detection of gases and vapors that can exert an injurious and toxic effect by leaking into the atmosphere during storage and use. Moreover, there is an increasing demand to directly and continuously monitor the concentrations of dangerous materials in the atmosphere and in water. Sensors for detecting and measuring the concentration of various chemical species in the atmosphere or in water are becoming a major area of interest in the electronics industry. Impedance-type gas sensors are based on resistivity and/or permittivity changes of conducting, semi-conducting and insulating polymers [31]. Intrinsically conducting polymers (ICP) can operate as sensors through the doping/dedoping of the polymer or through the entrapment of specific molecules.

A common characteristic of ICP such as polypyrrole (PPy) and polyaniline (PAni) is a one-dimensional organic backbone based on the alternation of single and double bonds, which enables a superorbital to be formed for electronic conduction. ICP are semiconducting in the neutral, undoped, state. The electrical conductivity increases significantly when electrons or holes are injected into the superorbital by introducing counter-ions, dopants, into the ICP [32]. Doping can change the conductivity by as much as 15 orders of magnitude—and the electrical properties can vary from insulator, to semiconductor to metal-like. There is, therefore, a range of conductivities from the dedoped state to the fully doped state. A reversible reaction that causes the polymer to change from one state to another, modifying the conductivity, can be used as an electrical switch. Among the principal advantages of PPy and PAni over other doped polymers are their excellent long term stability and their thermal stability in air [33,34]. The thin films of interest for sensor applications can be deposited using electro-deposition, chemical reaction, vapor phase reaction and even plasma polymerization [35]. Thin films can also be produced by casting subtly designed ICP-filled thermoplastic polymers which become conductive at very low ICP contents through the formation of a percolation network [36,37].

The sensor sensitivity can be enhanced by increasing the sensing surface area. Systems with enhanced surface areas include ICP-coatings on fabrics, cellular polymers and porous membranes [38–42]. The porous structure of a polyHIPE should allow the penetration of the ICP throughout and produce a conductive polyHIPE. Additional applications for such ICP-coated polyHIPE include antistatic packaging for microelectronic components and novel dielectric materials.

2. Experimental

2.1. Materials

The monomers used for the polyHIPE and the IPN synthesis were styrene (S, Fluka) and 2-ethylhexyl acrylate (EHA, Aldrich). The crosslinking comonomer was divinylbenzene (DVB, which includes 40% ethylstyrene isomers, Riedel-de Haen). The silicon-containing monomers for hybrid polyHIPE synthesis were organotrialkoxysilanes containing vinyl groups, methacryloxypropyltrimethoxysilane (MPS, Fluka) and vinyltrimethoxysilane (VS, Aldrich). All monomers except styrene and DVB were used without removing their inhibitors. The inhibitors in styrene and DVB were removed through extraction with 1.25 M NaOH (Carlo Erba). The initiators were potassium peroxodisulfate ($K_2S_2O_8$, water soluble, Riedel-de Haen) for HIPE polymerizations and benzoyl peroxide (BPO, monomer soluble, Fluka) for IPN polymerizations. The emulsifiers used (Sigma-Aldrich) had different hydrophilic lipoholic balances (HLB): sorbitan monooleate (SMO, Span 80, HLB = 4.3, less viscous) and sorbitan monolaurate (SML, Span 20, HLB = 8.6, more viscous). SML, with its higher HLB (8.6), was used in HIPE containing EHA to enhance the stability. SMO, with its lower HLB (4.3), was used for all the other HIPE. Calcium chloride hydrate ($CaCl_2 \cdot 2H_2O$, chemical pure, ACS, Israel) and K_2SO_4 (Frutarom, Israel) were the electrolytes used to stabilize the HIPE. The porogens used were toluene (T, Bio Lab) and heptane (H, Aldrich). Deionized water was used throughout.

The monomers used for the ICP were pyrrole (Py, Aldrich) and aniline (Ani, Aldrich). The oxidizing agent for

Table 1
HIPE compositions and polyHIPE densities

Type	Label	Composition, % (mass)	Density, g/cm^3
HIPE	S-a	90S/10DVB	0.11
	EHA/S-a	48EHA/36S/16DVB	0.11
HIPE with porogen	S-b+T	55(67S/33DVB):45T	0.05
IPN	IPN-3/1	75(EHA/S-a)+25(90S/10DVB)	0.10
	IPN-2/1	67(EHA/S-a)+33(90S/10DVB)	0.10
	IPN-1/1	50(EHA/S-a)+50(90S/10DVB)	0.11
	IPN-1/2	33(EHA/S-a)+67(90S/10DVB)	0.20
MPS hybrid with DVB	MPS-a-20	70S/10DVB/20MPS	0.09
	MPS-a-40	50S/10DVB/40MPS	0.10
	MPS-a-60	30S/10DVB/60MPS	0.11
	MPS-a-80	10S/10DVB/80MPS	0.12
MPS hybrid without DVB	MPS-b-10	90S/10MPS	0.19
	MPS-b-30	70S/30MPS	0.13
	MPS-b-50	50S/50MPS	0.10
	MPS-b-70	30S/70MPS	0.11
VS hybrid	VS-30	60S/10DVB/30VS	0.07
	VS-80	10S/10DVB/80VS	0.05
VS hybrid with porogen	VS-43+T	70(43S/14DVB/43VS):30T	0.06
	VS-43+H	70(43S/14DVB/43VS):30H	0.04

the Py polymerization was $FeCl_3$ (Riedel-de Haen) and the oxidizing agent for the Ani polymerization was ammonium persulfate (AP, Sigma). Dodecyl benzene sulfonic acid (DBSA, Aldrich) was added as an ICP dopant in some cases. The solvents used in the polyHIPE coating process were tetrahydrofuran (THF, Frutarom, Israel), methanol (MeOH, Bio Lab) and deionized water. Prior to coating, the polyHIPE were immersed in 0.001 M H_2SO_4 (Aldrich). The ICP-coated polyHIPE were used as sensors for the detection of acetone (Bio Lab) vapor.

2.2. PolyHIPE synthesis

A typical HIPE contained an aqueous phase with a mass fraction of approximately 0.883. The aqueous phase of the HIPE consisted of approximately 2.2% initiator and 5.5% electrolyte (by mass). A typical HIPE contained a monomer mass fraction of approximately 0.097 and an emulsifier mass fraction of approximately 0.020. The concentration of emulsifier was increased in order to enhance stability in HIPE containing VS and/or a porogen. The HIPE containing a high concentration of VS had a monomer mass fraction of approximately 0.096 and an emulsifier mass fraction of approximately 0.038. The HIPE containing a porogen had a monomer mass fraction of approximately 0.067, an emulsifier mass fraction of approximately 0.038, and a porogen mass fraction of 0.029. The HIPE compositions and polyHIPE densities for various systems are listed in Table 1. HIPE with relatively low monomer mass fractions produce polyHIPE with relatively low densities.

The polyHIPE synthesis has been described in detail elsewhere [9,10,23,29]. Briefly, the comonomers and emulsifier were stirred in a beaker for 5 min with a magnetic stirrer. Then, while stirring continued, the aqueous solution containing initiator and electrolyte was added slowly. The HIPE was placed in a convection oven at 60 °C overnight for polymerization. The water-filled polyHIPE was dried in a convection oven at 80 °C until a constant weight was achieved (about 24 h). The residual monomer, emulsifier, and porogen were removed from polyHIPE specimens using Soxhlet extraction in order to calculate the yield and to prepare the specimens for further processing and analysis. The Soxhlet extraction procedure was 24 h in deionized water followed by 24 h in methanol.

The overall polymerization yield for polyHIPE from HIPE containing organic (non-hybrid) monomers, $Y_{p,organic}$, was calculated using Eq. (1). The situation is slightly more complex when a hybrid monomer (silane) is included in the HIPE. The silane is expected to undergo hydrolysis and condensation reactions and, thus, the molecular weight of the silane in the polymer is different from the molecular weight of the silane monomer. It will be assumed that the hydrolysis and condensation reactions proceed to completion. An accurate description of the extent of condensation can be established using solid state NMR [27]. The overall polymerization yield for polyHIPE from HIPE containing a hybrid (silane) monomer, $Y_{p,hybrid}$, was calculated using Eq. (2).

$$Y_{p,organic} = \left(\frac{m_d m_a}{m_m m_b}\right) \times 100\% \quad (1)$$

$$Y_{p,hybrid} = \frac{m_d m_a}{m_b}\left(m_o + m_h\left(\frac{M_{full-HC}}{M_{no-HC}}\right)\right)^{-1} \times 100\% \quad (2)$$

where m_m is the mass of the monomers in the HIPE, m_d is the mass of the dried polyHIPE, m_b is the mass of a sample before extraction, m_a is the mass of a sample after extraction, m_o is the mass of the organic (non-hybrid) monomers in the HIPE, m_h is the mass of the hybrid (silane)

monomer in the HIPE, $M_{\text{no-HC}}$ is the molecular weight of the silane monomer and $M_{\text{full-HC}}$ is the molecular weight of the silane following hydrolysis and condensation reactions that proceed to completion.

2.3. IPN synthesis

The method used to synthesize an IPN within the polyHIPE is described in detail elsewhere [23]. Briefly, the IPN were prepared by taking the EHA/S-a polyHIPE (48EHA/36S/16DVB), swelling it with a monomer solution (88S/10DVB/2BPO) and, then, polymerizing and cross-linking at 70 °C for 24 h. The increase in the mass of the polyHIPE was approximately equal to the mass of the monomer mixture used to swell the polyHIPE. The compositions of the IPN based on EHA/S-a are listed in Table 1.

2.4. Silica monoliths

Silica monoliths were produced by pyrolysing the hybrid polyHIPE in nitrogen to a temperature of 600 °C and then holding in air at 600 °C for 1 h. The mass loss was determined by measuring the mass of the polyHIPE before pyrolysis and the mass of the silica monolith after pyrolysis. The shrinkage was determined by measuring the volume of the polyHIPE before pyrolysis and the volume of the silica monolith after pyrolysis.

2.5. ICP-coated polyHIPE

S-a (90S/10DVB) polyHIPE cubes, approximately $1\times 1\times 1$ cm^3, were coated with various ICP. Prior to coating, the polyHIPE surfaces were modified by immersion in an etchant, a 0.001 M solution of H_2SO_4, and then dried. The ICP coatings were based on the oxidative polymerization of either pyrrole or aniline. There were two different coating procedures used. In the first procedure, the polyHIPE was placed in an oxidant solution. The polyHIPE was then removed from the oxidant solution and dried, leaving oxidant on the polyHIPE cell surfaces. The polyHIPE was then immersed in a monomer solution under nitrogen for polymerization. The monomer reacted with the oxidant on the cell surfaces and polymerized, producing an ICP coating. The polyHIPE was then removed from the solution and dried. All the Py polymerizations were carried out in the dark. The compositions of the solutions and the immersion times in each solution were varied. In the second procedure, the polyHIPE was immersed in a monomer solution. The oxidant solution was then added to the monomer solution under nitrogen for polymerization. The compositions of the solutions and the immersion times in each solution were varied. The results from three different coating procedures will be described in this paper (Table 2).

2.6. Characterization

The densities of the polyHIPE were determined from weight and volume measurements. The specific surface areas of the polyHIPE were determined using the single-point BET (Brunauer, Emmett, Teller) method with nitrogen adsorption–desorption at 77 K (Flowsorb II, Micromeritics). The cellular structures of the polyHIPE were characterized from cryogenic fracture surfaces using high resolution scanning electron microscopy (HRSEM, LEO 982, Zeiss) with uncoated specimens and accelerating voltages of 1–2 kV. A stereo optical microscope was used to photograph the ICP-coated polyHIPE.

Dynamic mechanical thermal analysis (DMTA) temperature sweeps were performed in compression using a Rheometrics, MK III DMTA at a frequency of 1 Hz at 3 °C/min. The compressive stress–strain measurements were performed at 25 °C using the Rheometrics, MK III DMTA. The measurements were carried out until equipment-related force or displacement limitations were reached. The modulus of the polyHIPE was calculated from the stress–strain curve using the highest slope at low strains. The modulus for the bulk polymer, E_{polymer}, both for DMTA and static stress–strain, is related to the modulus of the polyHIPE, E_{polyHIPE}, using Eq. (3) [43].

$$E_{\text{polymer}} = E_{\text{polyHIPE}}\left(\frac{\rho_{\text{polymer}}}{\rho_{\text{polyHIPE}}}\right)^2 \tag{3}$$

where ρ_{polyHIPE} and ρ_{polymer} are the polyHIPE and polymer densities, respectively. The exact bulk densities of the copolymers in the polyHIPE are unknown, but are assumed to be quite similar and approximately 1 g/cm^3.

The thermal stability was characterized using thermogravimetric analysis (TGA) and differential thermal analysis (DTA) (TGA–DTA simultaneous analyzer, SDT2960, a module of TA INST 2000, TA-Instruments Company). PolyHIPE were run at 20 °C/min to 650 °C and beyond in a nitrogen environment (50 cm^3/min).

2.7. ICP-coated polyHIPE as a vapor sensor

The electrical properties (*IV* curves) were determined using a parallel plate current/voltage (*IV*) measurement apparatus in which the current is measured using an ammeter (Keithley 2000) as a function of the supplied voltage for a sample of area, A, and thickness, t. The resistance, R, is the inverse of the slope of the *IV* curve and the conductivity, σ, is $t/(RA)$. The surfaces of the coated polyHIPE cubes were covered with a relatively thick ICP layer. The surface layers were, therefore, removed prior to *IV* characterization. The sensing capabilities of the ICP-coated polyHIPE were determined by placing the cube with the skin removed on a wire mesh clamped to a retort stand. Pins were embedded into the opposite sides of the cube to a depth of 2 mm. The resistance between the pins was

Table 2
ICP coating procedures and the resulting conductivities

	PPy-a	PPy-b	PAni-a
Step 1	6 g $FeCl_3$; add THF to 25 ml; 12 h	0.687 ml Py; 8.03 g DBSA; add MeOH to 50 ml; 30 min	0.6 g Ani; 2.16 g DBSA; add H_2O to 60 ml; 48 h
Step 2	20 ml Py; 5 ml THF; 3 h	0.487 g $FeCl_3$; 50 ml H_2O; 3 h	1.5 AP; 5 g H_2O; 5 h
Color	Black	Brown	Green
ϕ_2	0.376	0.091	0.061
$\phi_2^{-3/2}$	4.3	36.6	66.6
$\sigma_{polyHIPE}$, S/m	20×10^{-4}	1×10^{-4}	–
σ_{PPy}, S/m	87×10^{-4}	37×10^{-4}	–

measured using clips attached to a multimeter (TES 2730, TES Electrical). The changes in resistance were measured as a beaker of acetone was placed under the retort stand and then removed. The exposure to acetone followed by the removal of acetone was repeated several times.

3. Results and discussion

3.1. PolyHIPE density and yield

The densities and compositions for the various polyHIPE investigated are listed in Table 1. Most of the HIPE that did not contain a porogen produced polyHIPE with densities of about 0.1 g/cm^3, as expected from the monomer mass fractions in the HIPE. Most of the IPN also had densities of about 0.1 g/cm^3, indicating that there was both an increase in volume (from swelling in S/DVB) and an increase in mass (from polymerization of S/DVB, which made the increase in volume permanent). The notable exceptions to densities of about 0.1 g/cm^3 are IPN-1/2 (0.20 g/cm^3 for 33(EHA/S-a)+67(90S/10DVB)), MPS-b-10 (0.19 g/cm^3 for 90S/10MPS) and the HIPE containing VS and/or a porogen (densities less than 0.07 g/cm^3, Table 1). The IPN synthesized using polyHIPE to monomer ratios that ranged from 3/1 to 1/1 exhibited the cellular structure typical of polyHIPE. IPN-1/2, however, exhibited fibrillar polystyrene inclusions within the polyHIPE cells [23]. The presence of these fibrillar polystyrene inclusions inside the normally empty cells produced the increase in density.

During polymerization, the integrity of the cellular HIPE structure is maintained against collapse through the formation of a stiff crosslinked polymer network. PolyHIPE without this stiff network can collapse during drying [23]. In non-hybrid polyHIPE, the crosslinking comonomer, DVB, forms a stiff organic network. In hybrid polyHIPE, an inorganic silsesquioxane network is formed through the hydrolysis and condensation of the methoxysilyl groups. MPS-b-10 contains no DVB and only 10% MPS and, therefore, the formation of a silsesquioxane network is limited by the low concentration of methoxysilyl groups. The relatively high density of MPS-b-10 reflects a partial collapse of the polyHIPE structure due to the limited development of a stiff network structure [29]. MPS-b-30 (70S/30MPS) and MPS-b-50 (50S/50MPS), contain significantly higher concentrations of silsesquioxane network-forming methoxysilyl groups and had densities of 0.13 and 0.10 g/cm^3, respectively.

The polymerization yields, $Y_{p,hybrid}$, were relatively low for some of the HIPE that contained VS (Table 3). The low yields reflect the low reactivity of VS [44]. In an MPS/S monomer mixture, both monomers tend to copolymerize [44]. In a VS/S monomer mixture, the VS is unlikely to homopolymerize, while the S tends to homopolymerize. As MPS is more reactive than VS, the yields from the MPS-containing HIPE are higher than those from the VS-containing HIPE [29,44]. Unreacted VS acts as a porogen and lowers the polyHIPE density.

In general the higher the VS concentration, the lower the yield, and the density. VS-30 (60S/10DVB/30VS) and VS-80 (10S/10DVB/80VS) have yields of 82 and 48%, respectively, and densities of 0.07 and 0.05 g/cm^3, respectively. The yield was significantly higher from HIPE that contained both VS and toluene (Table 3). The increase in yield most likely results from an enhanced molecular mobility in the toluene-swollen polymer that allows the free radical and condensation reactions to proceed to completion.

Porogens were added to some HIPE in order to increase the surface area and reduce the density. The density of S-b+T (0.05 g/cm^3, for 55(67S/33DVB):45T) reflects the mass fraction of monomer in the HIPE (0.06). The addition of a porogen also yielded a significant increase in surface area, from 29 m^2/g for S-a to 132 m^2/g for S-b+T [10]. The addition of a porogen to the HIPE containing VS enhanced the yield producing polyHIPE whose composition more closely resembled the monomer composition in the HIPE. The slight decrease in density on the addition of a porogen to a VS-containing HIPE (Table 3) reflects the combination of a reduction in density from the addition of a porogen and an increase in density from the increase in yield. A mass balance shows that the density of VS-43+T (0.06 g/cm^3, for 70(43S/14DVB/43VS):30T) is higher than that of VS-43+H (0.04 g/cm^3, for 70(43S/14DVB/43VS):30H) primarily because the yield is higher for VS-43+T (Table 3). Another factor influencing the polyHIPE density is the volume of

Table 3
VS-containing polyHIPE and silica monoliths

Label	m_{VS100}, % (mass)	$Y_{p,hybrid}$, % (mass)	Density, g/cm^3		Mass loss, % (mass)	Shrinkage, % (volume)	m_{VS}, % (mass)
			PolyHIPE	Silica			
S-a	–	92	0.11	–	100	–	–
VS-30	18	82	0.07	0.07	87	88	17
VS-80	68	48	0.05	0.05	60	62	53
VS-43+T	29	100	0.06	0.06	79	80	28
VS-43+H	29	83	0.04	0.05	84	85	21

porogen added. Since equal masses of porogen were added, the volume of toluene added was less than the volume of heptane added.

3.2. Mechanical properties and thermal stability

Two methods have been used to enhance the high temperature mechanical properties of polyHIPE, the formation of IPN based on polyHIPE and the synthesis of hybrid polyHIPE. The variation of tan δ with temperature for S-a, EHA/S-a and IPN-1/1 (50EHA/S-a+50(90S/10DVB)) are seen in Fig. 1. The tan δ peaks are 48 °C for EHA/S-a, 130 °C for IPN-1/1and 148 °C for S-a. It is not surprising that the tan δ peak for IPN-1/1 lies close to that of S-a, since IPN-1/1 contains a significant amount of crosslinked polystyrene. The tan δ peak temperatures for the polyHIPE are significantly higher than the literature values for T_g. This discrepancy reflects the extensive crosslinking in the polyHIPE as well as the polyHIPE's relatively low thermal conductivity which might produce a significant temperature difference between the sample and the thermocouple.

The different shapes of the tan δ curves are also of interest. S-a exhibits a high, narrow and relatively symmetric tan δ peak. Previous work has shown that for EHA/S copolymers, the height of the tan δ peak decreased and the breadth of the tan δ peak increased with increasing EHA content [23]. The relatively symmetric EHA/S-a tan δ peak in Fig. 1 is lower and broader than the tan δ peak for S-a. The synthesis of an IPN, however, yields a non-symmetric tan δ peak. Tan δ for IPN-1/1 begins to increase at about 40 °C, reaches a shoulder at about 74 °C, and remains at a relatively high tan δ over a relatively large temperature range. A comparison of the full width at half maximum (FWHM) of the tan δ peaks yields FWHM of 29, 59 and 92 °C for S-a, EHA/S-a and IPN-1/1, respectively. The relatively large FWHM of IPN-1/1 is typical of IPN. The phase-separated domains in the IPN can have a wide spectrum of compositions since phase separation is limited by the structure of intertwined networks. The IPN within a polyHIPE thus has a broader tan δ peak, extending the temperature range available for mechanical damping.

The bulk polymer E' were calculated from the polyHIPE E' using Eq. (3). The variations of bulk polymer E' with temperature for S-a, EHA/S-a and IPN-1/1 are seen in Fig. 2. At lower temperatures, the E' of the polymers are on the order of 1 GPa, as expected for polymers below their T_gs. Both S-a and EHA/S-a exhibit sharp reductions of two orders of magnitude in E' near their respective T_gs. The decrease in E' is more gradual for IPN-1/1, reflecting the wider damping temperature range of the IPN.

The effects of IPN formation on the compressive mechanical properties can be seen in the stress–strain curves in Fig. 3. EHA/S-a (Fig. 3(a)) exhibits a relatively low bulk polymer modulus (0.14 GPa) and reaches a plateau

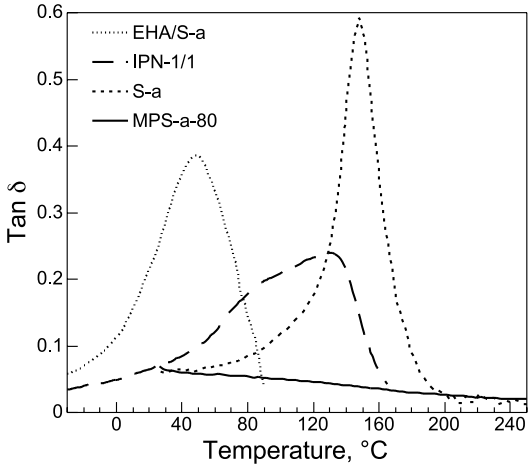

Fig. 1. Tan δ temperature sweep in compression for S-a, EHA/S-a, IPN-1/1 and MPS-a-80.

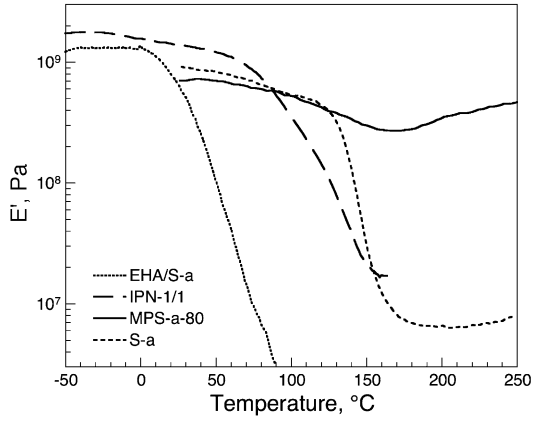

Fig. 2. E' of the bulk polymer from a temperature sweep in compression for S-a, EHA/S-a, IPN-1/1 and MPS-a-80.

stress at relatively low strains, reflecting a collapse of the cellular structure. When the compressive strain reaches 60% the collapse of the cellular structure reaches its limit and the stress begins to increase rapidly with increasing strain. IPN-1/1 has the EHA/S-a enmeshed within a polystyrene network and this is reflected in its compressive stress–strain curve in Fig. 3(b). The bulk polymer modulus (0.71 GPa) is significantly higher than that of EHA/S-a and there is only a trace of a shoulder, indicating that there is little collapse of the cellular structure. The compressive stress–strain curve of S-a (Fig. 3(c)) is somewhat similar to that of IPN-1/1. The bulk polymer modulus of S-a (1.22 GPa) is slightly higher than that of IPN-1/1 and there is no trace of a plateau or even a shoulder, indicating that there is no collapse of the cellular structure. The arrows indicate that the compressive stress–strain test was stopped since an apparatus related limitation was reached. Surprisingly, S-a did not fail in brittle fracture at a strain of 14%.

MPS-a-80 (10S/10DVB/80MPS) does not exhibit a tan δ peak in Fig. 1 and there is no significant decrease in the bulk polymer E' for MPS-a-80 in Fig. 2. There is little polystyrene segmental motion possible given the low styrene content and the severe restrictions on motion from the combined organic and inorganic networks. The extensively crosslinked silsesquioxane network is relatively unaffected by temperatures below 350 °C. The high temperature mechanical properties are, therefore, significantly enhanced through the formation of a hybrid polyHIPE.

S-a is glassy at 30 °C and exhibits a relatively high polymer modulus. MPS-a-80, Fig. 3(d), also exhibits a relatively high bulk polymer modulus (1.09 GPa). Unlike S-a, however, MPS-a-80 undergoes brittle fracture at a strain of 7%. The brittle fracture reflects the formation of a brittle highly crosslinked silsesquioxane network. The advantage of the silsesquioxane network can been seen in the compressive stress–strain curves at 250 °C. At 250 °C, S-a is rubbery (Fig. 3(e)). The bulk polymer modulus is 0.007 GPa and the cellular structure collapses at low stresses. MPS-a-80, however, exhibits a relatively high bulk polymer modulus at 250 °C (0.6 GPa), as indicated in Fig. 2. The characteristic mechanical properties of MPS-a-80 are relatively unchanged by exposure to 250 °C (Fig. 3(f)). Brittle fracture of MPS-a-80 at 250 °C occurs at a slightly higher strain and at a slightly lower stress than the brittle fracture at 30 °C.

The variation of the bulk polymer modulus in uniaxial compression with the MPS content for hybrid polyHIPE is seen in Fig. 4. At 30 °C, the bulk polymer moduli (about 1 GPa) for the MPS-a series, the hybrids with DVB, are relatively independent of the MPS content. At 250 °C, however, the bulk polymer moduli for the MPS-a series are strongly dependent on the MPS content (Fig. 4) since the organic network is above its T_g. The bulk polymer modulus increases from 0.007 GPa for S-a to 0.6 GPa for MPS-a-80. The silsesquioxane network maintains its rigidity at 250 °C and both its prevalence and its crosslink density increase with increasing MPS content. At 30 °C, the bulk polymer moduli for the MPS-b series, the hybrid polyHIPE without DVB, range from 0.4 to 0.6 GPa are lower than those of the hybrid polyHIPE with DVB and are dependent on the MPS content (Fig. 4). The lower moduli result from the absence of a stiff crosslinked organic network in the hybrid polyHIPE without DVB. As the stiff crosslinked networks in these materials are formed through the hydrolysis and condensation of the methoxysilyl groups, the modulus is, therefore, dependent on the MPS content.

The degradation of the polyHIPE is strongly affected by its composition, as seen in the TGA and DTA curves in Fig. 5 for the pyrolysis of S-a and MPS-a-80 in nitrogen. The mass loss and the size of the DTA peak in Fig. 5 are much greater for S-a than for MPS-a-80. The pyrolysis of an MPS-containing polyHIPE is expected to yield SiO_2. The higher the MPS content, the smaller the mass loss and the

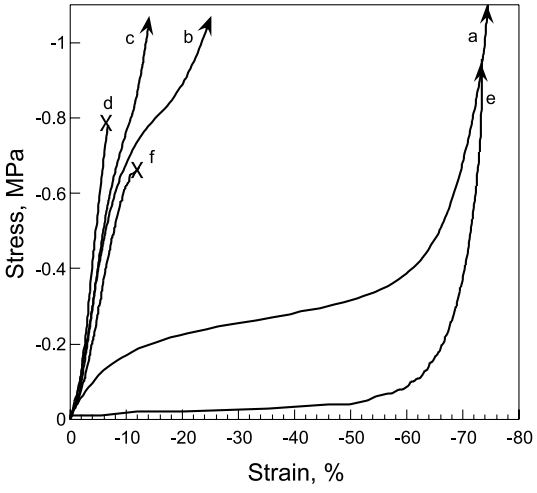

Fig. 3. Uniaxial compressive stress–strain curves in compression: (a) EHA/S-a, 30 °C; (b) IPN-1/1, 30 °C; (c) S-a, 30 °C; (d) MPS-a-80, 30 °C; (e) S-a, 250 °C; (f) MPS-a-80, 250 °C.

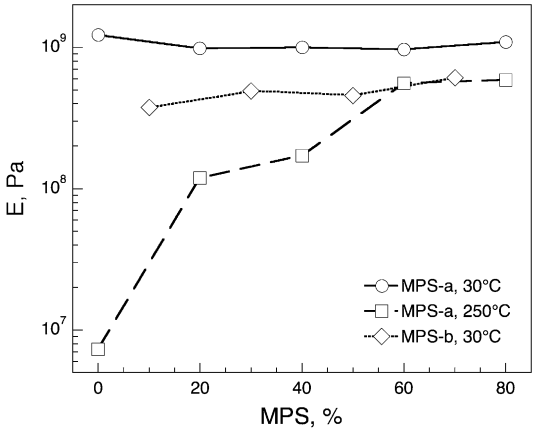

Fig. 4. Variation of the bulk polymer's uniaxial compressive modulus with MPS content for the MPS-a series (hybrids with DVB) at 30 and 250 °C and for the MPS-b series (hybrids without DVB) at 30 °C.

smaller the exothermic pyrolysis peak. The relatively linear increase in residual mass with MPS content is seen in Fig. 6. The DTA peak temperature for MPS-a-80 in Fig. 5, is less than the DTA peak temperature for S-a. An almost linear decrease in DTA peak temperature with MPS content is seen in Fig. 6. The TGA and DTA curves in Fig. 5 indicate that the degradation of MPS-a-80 begins at a lower temperature than the degradation of S-a. The reduction in the onset of degradation and in the DTA peak temperature on the addition of MPS results from the methacrylate group that is less thermally stable than styrene [45]. Silanes that do not contain a methacrylate group, such as VS, should not cause a reduction in the thermal degradation onset temperature.

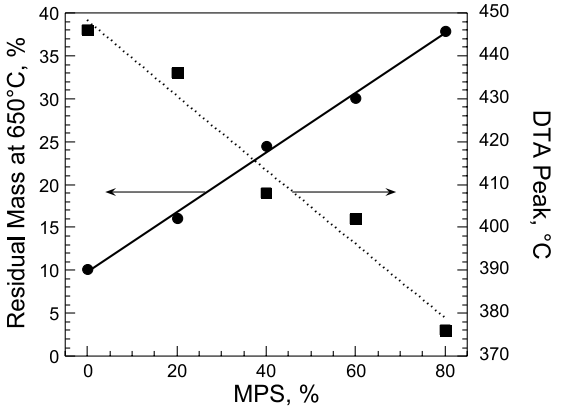

Fig. 6. Variation of residual mass and DTA peak position with MPS content.

3.3. VS-containing polyHIPE and silica monoliths

Silica monoliths were produced through the pyrolysis of the VS-containing polyHIPE listed in Table 3. VS-30 exhibited a mass loss of approximately 87% and a shrinkage of approximately 88% on pyrolysis. VS-80 had a significantly greater VS content in the monomer and, therefore, exhibited a smaller mass loss (60%) and a smaller shrinkage (62%) than VS-30. The overall volume shrinkage was similar to the mass loss for all the VS-containing polyHIPE (Table 3). Since the volume loss and mass loss were similar, the densities of the pyrolysed monoliths were similar to the densities of the polyHIPE. However, the density of silica is more than twice the density of the polymer, and this indicates that the volume fraction of silica in the monolith is less than half of the volume fraction of polymer in the polyHIPE.

The mass percentage of VS that would be expected from a polyHIPE reaction that reached 100% completion, m_{VS100}, is listed in Table 3. m_{VS100} was calculated from the monomer composition by assuming that the free radical reaction reached completion (100% yield) and by assuming that the hydrolysis and condensation reactions reached completion (yielding $C_2H_3SiO_{1.5}$). m_{VS100} is less than the mass percent in the monomer mixture, reflecting the change in molecular weight (148 g/mol before hydrolysis and condensation, 79 g/mol following complete hydrolysis and condensation). An estimate for the amount of VS incorporated into the polyHIPE, m_{VS}, was calculated from the pyrolysis residual mass (Table 3). m_{VS} was calculated by assuming that the pyrolysis yields SiO_2 only, that the SiO_2 includes all the silicon present in the polyHIPE, and that the hydrolysis and condensation reactions reached completion (yielding $C_2H_3SiO_{1.5}$). A comparison of m_{VS} and m_{VS100} indicates that for VS-30 and VS-43+T the percentage of VS in the polymer is similar to that expected from the monomer composition. The m_{VS} are relatively low for VS-80 and VS-43+H, indicating that there was a significant amount of VS that acted as porogen and produced low densities. The relatively low VS conversion for VS-80 (about 77%) most likely reflects the low VS reactivity at high VS contents. The relatively low VS conversion for VS-43+H (about 73%) may reflect the effects of heptane's solubility parameter [46,47], which is less than that of the polymer, limiting the swelling and the enhancement of molecular mobility. The relatively low VS conversion may also reflect the effects of heptane's chain transfer constant [48], which is higher than that of toluene and may impede polymerization.

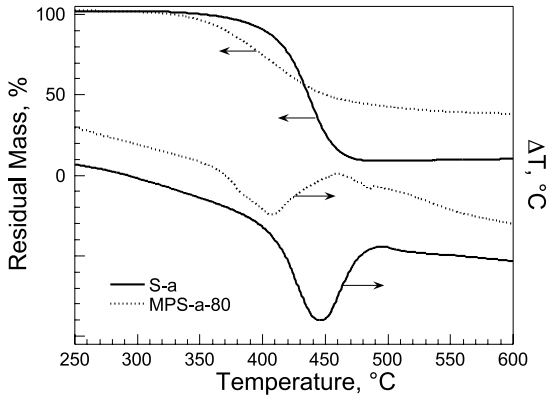

Fig. 5. DTG and DTA temperature sweeps in N_2 for S-a and MPS-a-80.

The cellular structure of S-a is seen in Fig. 7(a). The cells are 15–25 μm in diameter and are connected by intercellular pores 0.5–10 μm in diameter. The struts in the cell walls have smooth, uniform surfaces, as seen in Fig. 7(b). The cells in VS-30 and VS-80 can be as large as 70 μm, significantly larger than the cells in S-a. Although the cellular structure of a particular area of VS-30 (Fig. 7(c)) may seem denser than that of S-a, the VS polyHIPE are less dense than S-a owing to the presence of the very large cells and the presence of unreacted VS. The cell walls of the VS polyHIPE, Fig. 7(d), are not as smooth and uniform as those in S-a, resulting from the unpolymerized VS which acted like a porogen. The cellular structure of the silica monolith from the pyrolysis of VS-30, Fig. 7(e) and (f), is similar to that of VS-30 in Fig. 7(c) and (d).

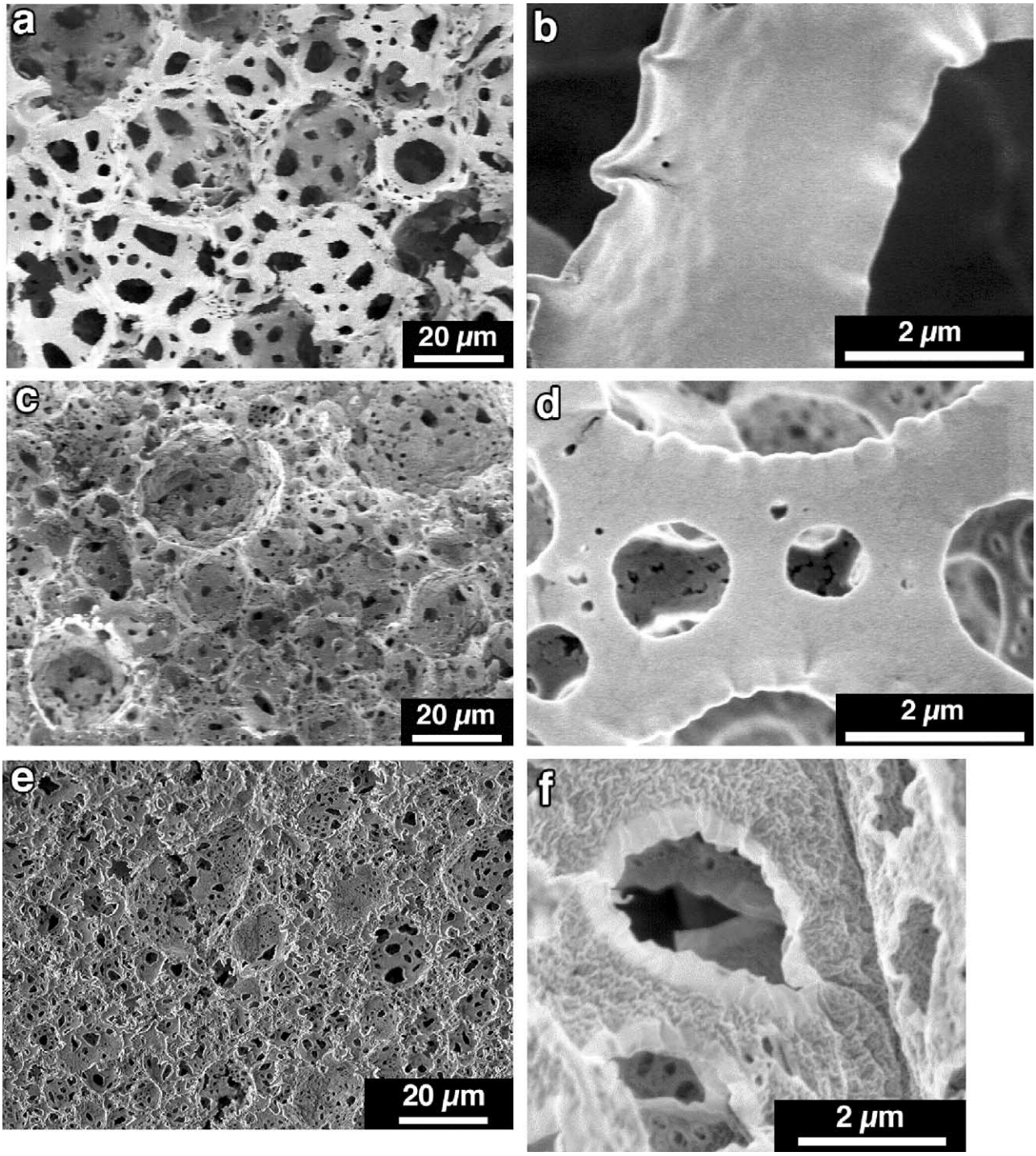

Fig. 7. SEM micrographs of polyHIPE and silica monoliths: (a) and (b) S-a; (c) and (d) VS-30; (e) and (f) silica monolith from VS-30; (g) and (h) VS-43+T; (i) and (j) silica monolith from VS-43+T.

The addition of a porogen to the HIPE has a significant effect on the cellular structure. The cellular structures of VS-30+T, Fig. 7(g), and of VS-30+H (not shown) are reminiscent of foaming soap bubbles. The cells are more circular in appearance and the struts contain relatively large pores. The struts for VS-30+T, Fig. 7(h), have a highly porous nanoscale structure. This cellular structure is maintained in the silica monoliths from the pyrolysis of VS-30+T (Fig. 7(i) and (j)) and VS-30+H (not shown).

3.4. PolyHIPE sensors

The centers of the polyHIPE cubes that were coated using the procedures in Table 2 exhibited conductivity,

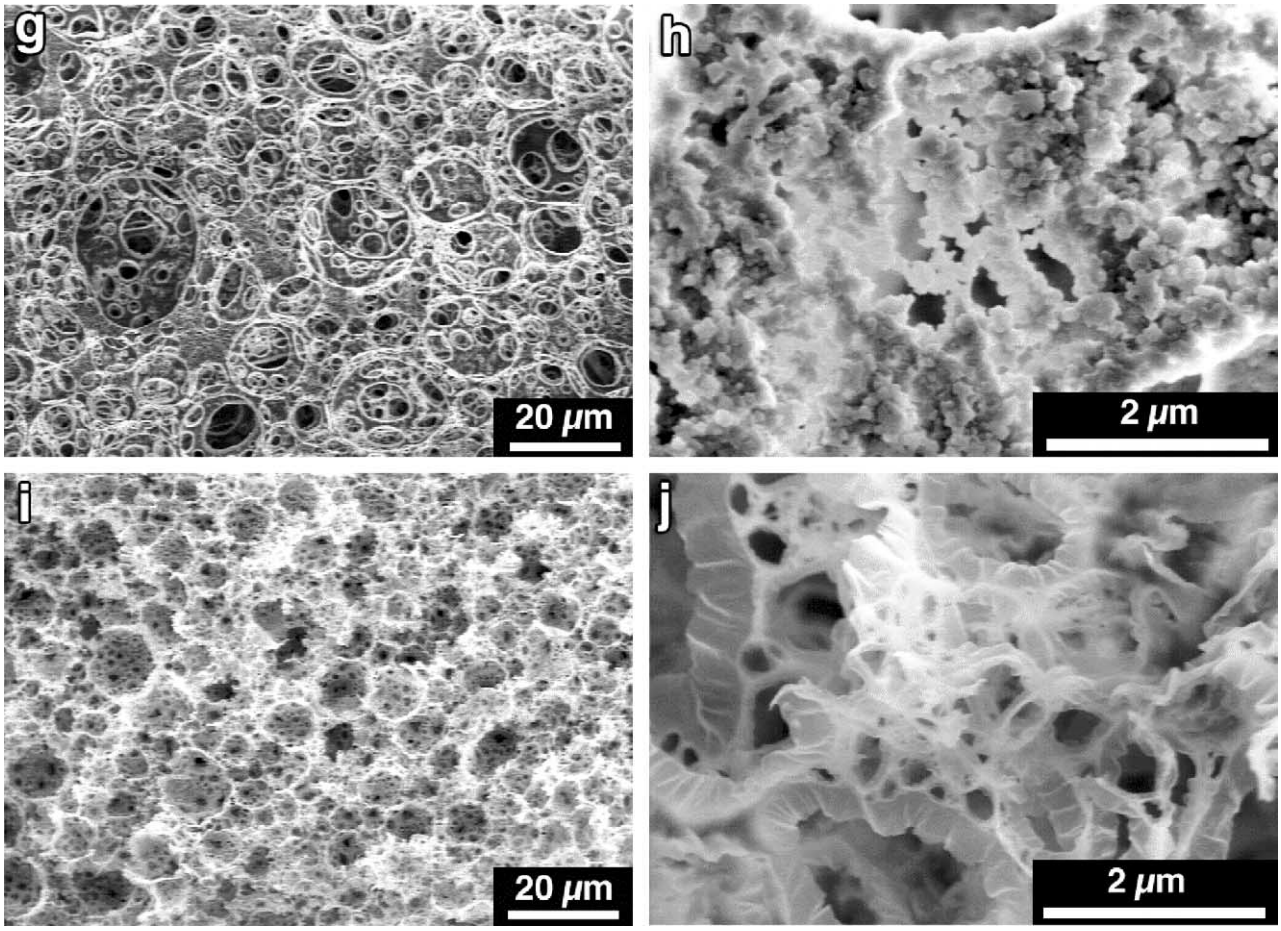

Fig. 7 (*continued*)

unlike the original S-a. The monomer, solvent and procedure (monomer first or oxidant first) used in the ICP coating process made significant differences in the quality of the coating and in the resulting conductivity. The color of the S-a cube cross-section is white (Fig. 8(a)). The S-a cube was coated throughout with a black PPy coating (Fig. 8(b)) when THF was the solvent and the pyrrole was used in the second step (PPy-a, Table 2). S-a was swollen by THF using the PPy-a procedure (Table 2). On drying, the cube was warped, the cellular structure was warped (Fig. 9), and the overall volume was slightly reduced. The S-a cube was coated throughout with a brown, less conductive PPy coating while the surface was coated with a black skin (Fig. 8(c)) when methanol was the solvent and pyrrole was used in the first step (PPy-b, Table 2). The cube shape and cellular structure were unaltered when using the PPy-b procedure. The S-a cube exhibited a dark green PAni skin on the outside tapering off to whitish at the center (Fig. 8(d)) using the PAni-a coating procedure (Table 2). The whitish area at the center did, however, exhibit conductivity, in spite of the lack of a visible green coating. Spectra from the center (not shown), taken using photo-acoustic Fourier transform infrared spectroscopy (FTIR, Bruker Equinox 55), exhibited the distinct peaks associated with PAni. These results indicate the presence of a PAni coating throughout the sample.

The polyHIPE coated with PPy-a and PPy-b exhibited ohmic behavior. The PPy-a yielded superior polyHIPE conductivity, as seen in the polyHIPE *IV* behavior (Fig. 10). The conductivities of the polyHIPE, σ_{polyHIPE}, were 20×10^{-4} S/m for the PPy-a coating and 1×10^{-4} S/m for the PPy-b coating. This significant difference reflects not only the differences in the PPy but also the differences in the coating. The conductivity of a porous material is expected to be significantly less than the conductivity of the bulk due to both the reduction in contact area and the increase in conducting path tortuousity. The conductivity of the PPy that is coating the polyHIPE, σ_{PPy}, can be related to the measured conductivity of the polyHIPE, σ_{polyHIPE}, using Eq. (4), which is based on the relationship between metal foam conductivity and bulk metal conductivity [43]:

$$\sigma_{\text{PPy}} = \sigma_{\text{polyHIPE}}\phi_2^{-3/2} \tag{4}$$

where ϕ_2 is the volume fraction of the metal in the foam. This can be applied to the polyHIPE if ϕ_2 is taken to be the volume fraction of the ICP film which forms a conformal coating on the polyHIPE. The ICP ϕ_2 can be calculated using Eq. (5):

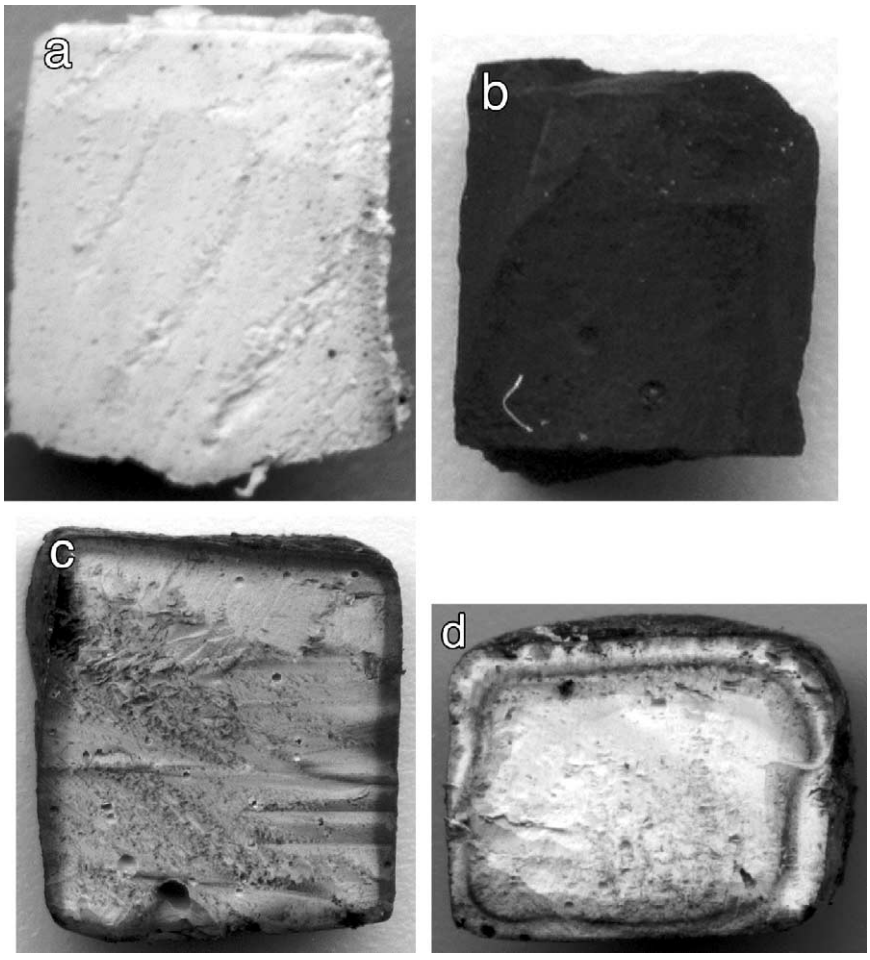

Fig. 8. OM micrographs of ICP-coated S-a cube (approximately $1\times1\times1$ cm^3) cross-sections: (a) uncoated, white; (b) PPy-a, black; (c) PPy-b, brown; (d) PAni-a, green.

$$\phi_2 = \frac{m_{\mathrm{PPy}}/\rho_{\mathrm{PPy}}}{V} \tag{5}$$

where m_{PPy} is the measured mass of the PPy coating, V, is the measured volume of the cube, and, ρ_{PPy} is the density of PPy, 1.3 g/cm^3. The PPy conductivities, σ_{PPy}, calculated using Eqs. (4) and (5) are 87×10^{-4} and 40×10^{-4} S/m for PPy-a and PPy-b, respectively. This difference is significantly smaller than the difference between the $\sigma_{\mathrm{polyHIPE}}$ since σ_{PPy} takes into account the significantly greater volume fraction of PPy in PPy-a.

Exposure to an organic vapor affected the conductivity.

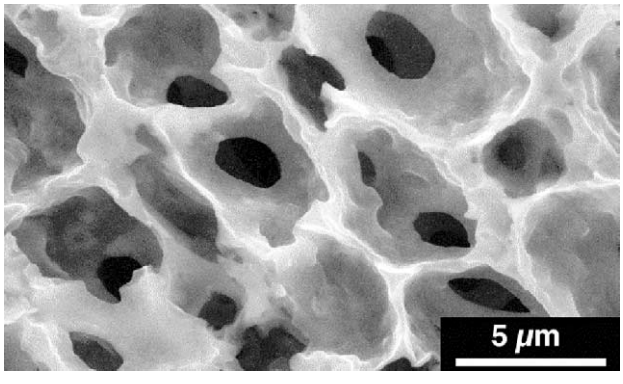

Fig. 9. SEM micrograph of a cross-section of S-a coated with PPy-a.

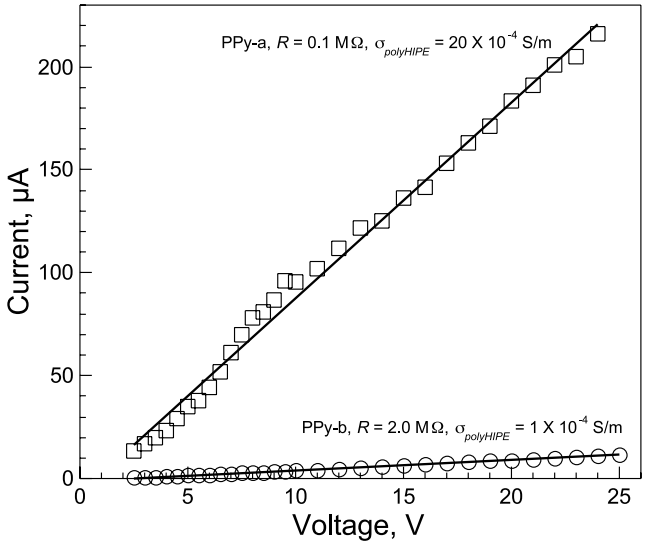

Fig. 10. *I–V* curves for S-a coated with either PPy-a or PPy-b.

Within a few seconds of exposure to acetone vapor, the PPy-b conductivity increased by a factor of five. When the acetone source was removed, the conductivity decreased and returned to its original value. These changes in conductivity were reversible and repeatable and demonstrated that using ICP-coated polyHIPE as sensors for organic vapors is feasible.

4. Conclusions

Various polyHIPE systems were investigated: IPN from polyHIPE, hybrid polyHIPE, silica monoliths from hybrid polyHIPE, and ICP-coated polyHIPE. A typical polyHIPE had a density of about 0.1 g/cm^3 and a cellular structure with cells 15–25 μm in diameter connected by intercellular pores 0.5–10 μm in diameter.

- IPN with densities of about 0.1 g/cm^3 resulted when the mass of the polyHIPE was greater or equal to the mass of the monomer added. IPN-1/1 had superior mechanical properties at higher temperatures and a relatively broad tan δ damping peak.
- The high temperature mechanical properties were improved dramatically through the synthesis of hybrid polyHIPE containing an inorganic silsesquioxane network. The moduli of the polyHIPE at 250 °C were dependent on the MPS content. The moduli at 30 °C were independent of the MPS content in the presence of a stiff organic network and dependent on the MPS content in the absence of a stiff organic network.
- The use of a porogen and/or the relatively low yield from the polymerization of VS yielded polyHIPE with lower densities. The use of a porogen in S-b+T yielded a relatively low density (0.05 g/cm^3), a nanoscale porous structure in the cell walls and a relatively high specific surface area (132 m^2/g). The presence of toluene in the VS-containing HIPE produced an increase in yield, a reduction in density, and a cellular structure unlike those of the other polyHIPE.
- Silica monoliths from the pyrolysis of VS-containing hybrid polyHIPE exhibited cellular structures similar to those of the original polyHIPE. The densities of the silica monoliths were similar to those of the polyHIPE, indicating that the volume fractions of silica in the monoliths could be as low as 0.02.
- The polyHIPE cubes were coated throughout with conductive PPy or PAni. The conductivities of the polyHIPE (1 to 20×10^{-4} S/m) were used to calculate the conductivities of the PPy coatings (37 to 87×10^{-4} S/m). The PPy-coated polyHIPE exhibited reversible and repeatable changes in conductivity when exposed to acetone vapor.

Acknowledgements

The TGA–DTA measurements were performed by Ms Ji Rongqin of Hebei University of Technology, and her assistance is gratefully acknowledged. The partial support of the Technion VPR Fund and the Goldsmith Visiting Scientist Fund are gratefully acknowledged.

References

[1] Lissant KJ. Emulsions and emulsion technology, part 1. New York: Marcel Dekker; 1974 [chapter 1].
[2] Cameron NR, Sherrington DC. Adv Polym Sci 1996;126:163.
[3] Barby D, Haq Z. US Patent 4,522,953; 1985.
[4] Shach-Caplan M, Narkis M, Silverstein MS. Polym Adv Technol 2003;14:83.
[5] Shach-Caplan M, Narkis M, Silverstein MS. J Polym Eng 2003;22:417.
[6] Desmarais TA. PCT Int Appl WO 9947183l; 1999.
[7] Dyer JC, Lioyd SN. PCT Int Appl WO 9621682; 1996.
[8] Mork SW, Rose GD. PCT Int Appl WO 9718246; 1997.
[9] Sergienko AY, Tai H, Narkis M, Silverstein MS. J Appl Polym Sci 2002;84:2018.
[10] Sergienko AY, Tai H, Narkis M, Silverstein MS. J Appl Polym Sci 2004;94:2233.
[11] Benicewicz BC, Jarvinen GD, Kathios DJ, Jorgensen BS. J Radioanal Nucl Chem 1998;235(1–2):31.
[12] Wakeman RJ, Bhumgara ZG, Akay G. Chem Eng J 1998;70:133.
[13] Hoisington MA, Duke JR, Apen PG. Polym Mater Sci Eng 1996;74:240.
[14] Hoisington MA, Duke JR, Langlois DA. Mater Res Soc Symp Proc 1996;431:539.
[15] Hoisington MA, Duke JR, Apen PG. Polymer 1997;38:3347.
[16] Duke JR, Hoisington MA, Langlois DA, Benicewicz BC. Polymer 1998;39:4369.
[17] Sperling LH. Polymeric multicomponent materials. New York: Wiley; 1997.
[18] Klempner D, Sperling LH, Utracki LA. Interpenetrating polymer networks. Advances in chemistry series. vol. 239. Washington, DC: American Chemical Society; 1994.
[19] Silverstein MS, Narkis M. Polym Eng Sci 1985;25:257.
[20] Narkis M, Talmon Y, Silverstein MS. Polymer 1985;26:1359.
[21] Silverstein MS, Narkis M. J Appl Polym Sci 1987;33:2529.
[22] Silverstein MS, Narkis M. Polym Eng Sci 1989;29:824.
[23] Tai H, Sergienko A, Silverstein MS. Polym Eng Sci 2001;41:1540.
[24] Cameron NR, Sherrington DC. Macromolecules 1997;30:5860.
[25] Zhu B, Katsoulis DE, Keryk JR, McGarry FJ. Polymer 2000;41:7559.
[26] Loy DA, Schneider DA, Baugher BM, Rahimian K. Book of abstracts, 219th ACS national meeting, San Francisco, CA; March 26—30, 2000.
[27] Sluzney A, Silverstein MS, Kababya S, Schmidt A, Narkis M. J Polym Sci, Polym Chem 2001;39:8.
[28] Sluzney A, Silverstein MS, Narkis N, Narkis M. J Appl Polym Sci 2001;81:1429.
[29] Tai H, Sergienko A, Silverstein MS. Polymer 2001;42:4473.
[30] Tai HW, Shea K, Silverstein M. PMSE Proc 2002;86:235.
[31] Harsanyi G. Polymer films in sensor applications. Lancaster: Technomic Publishing; 1995.
[32] Young RJ. Plast Rubber Int 1984;9:29.
[33] Sethi RS, Goosey MT. In: Chilton JA, Goosey MT, editors. Special polymers for electronics and optoelectronics. London: Chapman&Hall; 1995.
[34] Wynne KJ, Street GB. Macromolecules 1985;18:2361.
[35] Silverstein MS, Visoly I. Polymer 2001;43:11.
[36] Roichman Y, Titelman G, Silverstein MS, Siegmann A, Narkis M. Synth Met 1999;98:201.

[37] Roichman Y, Silverstein MS, Siegmann A, Narkis M. J Macromol Phys 1999;B38:145.
[38] Collins GE, Buckley LJ. Synth Met 1996;78:93.
[39] Kincal D, Kumar A, Child AD, Reynolds JR. Synth Met 1998;92:53.
[40] Fu Y, Weiss RA, Gan PP, Bessette MD. Polym Eng Sci 1998;38:857.
[41] Sotzing GA, Scruggs NR, Wang Y, Carignan J, Weiss RA. Polym Prepr 2001;42:284.
[42] Frisch HL, Ma J, Song H, Frisch KC, Mengnjoh PC, Molla AH. J Appl Polym Sci 2001;80:893.
[43] Gibson LJ, Ashby MF. Cellular solids, structure and properties. 2nd ed. Oxford: Pergamon Press; 1997.
[44] Greenley RZ. In: Brandrup J, Immergut EH, Grulke EA, editors. Polymer handbook. 4th ed. New York: Wiley; 1999. p. II/181.
[45] Chartoff RP. In: Turi EA, editor. Thermal characterization of polymeric materials. New York: Academic Press; 1997.
[46] Du Y, Xue Y, Frisch HL. In: Mark JE, editor. Physical properties of polymers handbook. New York: American Institute of Physics; 1996. p. 227.
[47] Grulke EA. In: Brandrup J, Immergut EH, Grulke EA, editors. Polymer handbook. 4th ed. New York: Wiley; 1999. p. VII/675.
[48] Ueda A, Nagai S. In: Brandrup J, Immergut EH, Grulke EA, editors. Polymer handbook. 4th ed. New York: Wiley; 1999. p. II/97.